

Superconducting Gap in Bi-Sr-Ca-Cu-O by High-Resolution Angle-Resolved Photoelectron Spectroscopy

C. G. OLSON, R. LIU, A.-B. YANG, D. W. LYNCH, A. J. ARKO, R. S. LIST, B. W. VEAL, Y. C. CHANG, P. Z. JIANG, A. P. PAULIKAS

Detailed studies indicate a superconducting gap in the high-temperature superconductor $\text{Bi}_2\text{Sr}_2\text{CaCu}_2\text{O}_8$. Photoemission measurements with high energy and angle resolution isolate the behavior of a single band as it crosses the Fermi level in both the normal and superconducting states, giving support to the Fermi liquid picture. The magnitude of the gap is 24 millielectron volts.

THE GAP AT THE FERMI LEVEL IS A fundamental property of any superconductor, and one of great interest for the new classes of high critical temperature (T_c) superconductors. Early direct measurements were made by far infrared absorption and tunneling. For all classes of the new high T_c materials the results for 2Δ , the gap energy, scattered considerably in the range of about 3 to 11 times kT_c (where k is Boltzmann's constant), mostly larger than the $3.52kT_c$ expected from the weak-coupling Bardeen-Cooper-Schrieffer (BCS) theory. Inhomogeneous samples and the difficulty in making contacts probably caused much of the scatter in the tunneling measurements, and the large anisotropy of the dielectric function probably led to difficul-

ties in the infrared measurements. Early attempts to detect the gap by photoelectron spectroscopy were generally inconclusive, owing to poor sample surfaces and inadequate resolution. More recently Imer *et al.* (1) reported measurements with high electron energy resolution that indicated a gap of $\Delta = 30$ meV. The angle integration and the necessity of repeatedly preparing fresh surfaces precluded comparison of a single part of the zone in the normal and superconducting states. Since then, Manzke *et al.* (2) have reported measurements with high angle resolution (hence, high wave vector, k , resolution) and moderate energy resolution. They also report a 30-meV gap.

In the high angle- and energy-resolution measurements reported here, we isolate the behavior of the states in a single band near the Fermi level in both the superconducting and normal states as a function of angle, and in addition, study the effect of temperature on the superconducting gap. We find a gap of $\Delta = 24$ meV, somewhat smaller than that

reported earlier, but still twice that of the weak-coupling BCS value ($2\Delta/kT_c$ of 7.0 versus 3.52).

A single crystal of $\text{Bi}_2\text{Sr}_2\text{CaCu}_2\text{O}_8$ was cleaved at 20 K in a vacuum better than 5×10^{-11} Torr. The surface was a (001) plane. Previous work with the 1-2-3 compounds (3, 4) showed that oxygen could easily be lost at 50 K from the surface layers sampled by photoelectron spectroscopy, but the Bi compounds proved to be much more stable. The data to be reported were taken first at 20 K after cleaving (5) but they were reproduced upon cooling back to 20 K after measurements at temperatures up to 100 K. The sample used had a value of T_c of 82 K determined from magnetic susceptibility measurements. Photons were provided by the Ames/Montana ERG/Seya beam line (6) on Aladdin, and we used the Seya in the 15- to 25-eV region. The instrument function of the monochromator was measured. It is approximately Gaussian, with an asymmetric tail to the low binding energy side of the energy distribution curves (EDCs) shown. The full width at half maximum (FWHM) is 24 meV for 22-eV photons. The photoelectrons were energy analyzed by a 50-mm radius hemispherical analyzer mounted on a goniometer (Vacuum Science Workshops). The analyzer instrument function was Gaussian, with a FWHM of 20 meV at the pass energy of 2 eV. The combined instrument function (FWHM ≈ 32 meV) was verified by comparison to a metallic Fermi level at 20 K. The analyzer input lens had an angular acceptance of about 2° . The value and stability of the instrument Fermi level were monitored by means of a clean Pt foil mounted on the refrigerator next to the sample. In the spectra to be reported the energy scale is that of the initial state ("binding energy").

C. G. Olson, R. Liu, A.-B. Yang, D. W. Lynch, Department of Physics and Ames Laboratory, USDOE, Iowa State University, Ames, IA 50010.
A. J. Arko and R. S. List, Los Alamos National Laboratory, Los Alamos, NM 87545.
B. W. Veal, Y. C. Chang, P. Z. Jiang, A. P. Paulikas, Argonne National Laboratory, Argonne, IL 60439.

Fig. 1. (A) Angle-resolved energy distribution curves for a surface of $\text{Bi}_2\text{Sr}_2\text{Ca}_1\text{Cu}_2\text{O}_8$ cleaved at 20 K, but measured at 90 K. The electron emission angles are marked. The inset shows schematically the motion of the initial state as the emission angle is changed. (B) Angle-resolved energy distribution curves for the sample cleaved and measured at 20 K (heavier lines), with the 90 K spectra superimposed with lighter lines. (C) Angle-resolved energy distribution curves for the surface taken at 15° at several temperatures below T_c and one above.

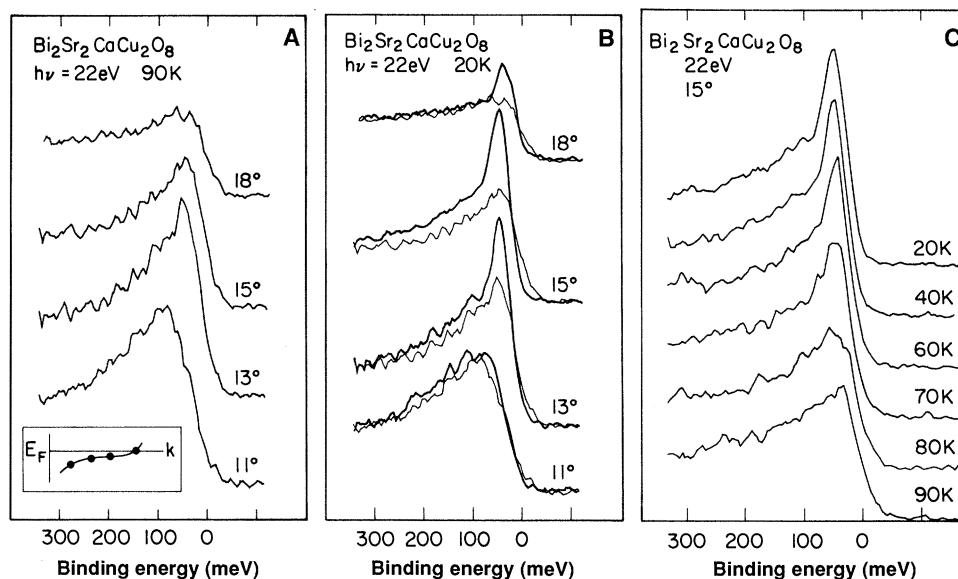


Figure 1A shows EDCs taken at different emission angles, hence different directions in \mathbf{k} -space, at a temperature above T_c . The direction sampled is nearly parallel to the zone diagonal Γ -M. However, we want to emphasize the temperature dependence of the spectra. Any detailed comparison to a specific model or calculation requires a much larger data set. The important thing to note in Fig. 1A is that at 11° the band is well below the Fermi level, and that there is very little strength at E_F . As we move out in the Brillouin zone, the band approaches the Fermi level, then stays parallel to, but below, E_F . Finally, in the 18° spectrum, the band crosses the Fermi level. For this direction, there is a filled density of states up to the Fermi level for temperatures above T_c . The inset in Fig. 1A is a schematic representation of the band.

Figure 1B shows EDCs taken at 20 K with the sample in the superconducting state, with the normal state spectra of Fig. 1A superimposed. The effect of opening a superconducting gap is apparent. At 11° , where the band is well below E_F , there is only a slight sharpening of the band with reduced temperature. In the other spectra, the density of states has weakened at E_F and piles up at slightly deeper binding energies. Indeed, the apparent strength remaining at E_F is the result of the asymmetric instrument function mentioned above.

The changes shown in Fig. 1B are reversible and repeatable on the same surface. $\text{Bi}_2\text{Sr}_2\text{CaCu}_2\text{O}_8$ is sufficiently stable that by minimizing the time and temperature in the normal state, the sample surface showed no degradation over the duration of the measurements. Spectra were also taken as a function of temperature to ensure that the changes were a result of the superconducting transition, and not simply a temperature effect. In Fig. 1C, the sample temperature was increased in steps, then stabilized while the spectra were taken. It is clear that the changes are related to the superconducting

transition. A more detailed comparison to the theoretical temperature dependence will be made in the next section.

The superconducting gap cannot be determined directly from Fig. 1B. The measured spectrum is a function of the normal state density of states (in \mathbf{k} -space), and the Fermi-Dirac distribution function, the modifications due to the gap, and the convolution with the instrument function. To model the spectrum, we began with the simplest case, the 90 K spectrum at 18° . A Lorentzian was used to represent the intrinsic spectrum and a linear function was used for the region at greater binding energy. (The linear portion extended to the Fermi energy.) The width of the Lorentzian is expected to result from the photoelectron lifetime width, with a possible small contribution from the dispersion of the initial- and final-state bands (7). This width and the position of the peak are the important unknown parameters in the fit. The Lorentzian and linear term were multiplied by a 90 K Fermi function and convolved with the monochromator and analyzer instrument functions. The fit shown in Fig. 2 resulted. Then this Lorentzian and linear term were used to fit the 20 K spectrum by multiplying their sum by a BCS density of states (not strictly correct, but no better method yet exists) and a 20 K Fermi function. The Lorentzian peak position was not shifted. This was then convolved with the instrument function. An excellent fit of the edge could be obtained for a small range of values of Δ , but the calculated spectrum did not peak as high as the measured one. By reducing the value of the Lorentzian width, a physically reasonable procedure because there will be less electron-electron scattering with a gap present, the excellent fit of Fig. 2 was obtained. This fit deteriorated noticeably whenever Δ fell out of the range 22 to 26 meV. A value for Δ of 24 meV gives $2\Delta = 7.0kT_c$.

The data at 18° were taken only at 20 and

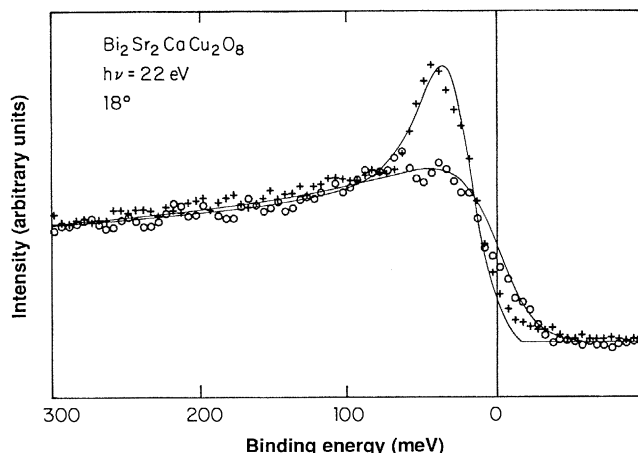


Fig. 2. Angle-resolved energy distribution curve for the surface of Fig. 1 taken at an angle of 18° at temperatures above and below T_c . The solid curves are the fits to the model described in the text. The binding energy of the Lorentzian is 33 meV and its width is 75 meV at 90 K and 40 meV at 20 K.

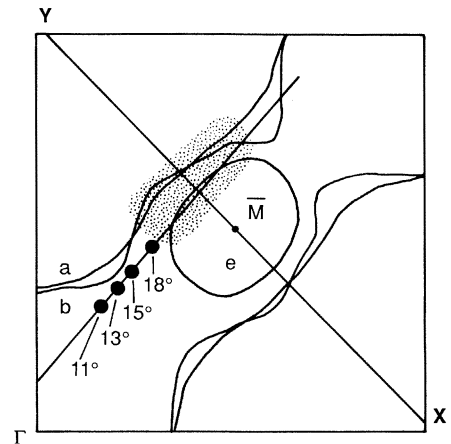


Fig. 3. Section through the center of the Brillouin zone with the calculated Fermi surface from Shen *et al.* (16). The letters and shading denote wave function admixtures (see text). The regions of the zone sampled by our measurements are indicated by the four dots.

90 K. The data taken at 15° were taken at many temperatures (Fig. 1C). However, at this angle the EDC peak is clearly below the Fermi level in the 90 K spectrum. When fitting it with a Lorentzian, the peak was found to be 55 meV below E_F , instead of the 33 meV for the 18° spectra of Fig. 2. As a result, a different value of Δ , 34 meV resulted. This should not be taken as evidence for gap anisotropy, but rather is an inadequacy of the model when the EDC peak moves away from E_F . The value of 34 meV obtained from the 15° data is closer to the results of Imer *et al.* (1) and Manzke *et al.* (2), but we believe that the errors in Δ by modeling grow as the band moves further from E_F , where the gap has a smaller influence on the spectrum.

Tunneling measurements of Δ have been reported (8). The low-temperature value was 25 meV, and the temperature dependence measured. The values of Δ versus T followed, within errors, the BCS weak-coupling expectation. Unlike the tunneling measurements, the temperature dependence shown in Fig. 1C is consistent with the strong coupling predicted by a value of 7 for $2\Delta/kT_c$. The gap does not decrease as rapidly with temperature as in the weak-coupling case, because it is less likely that an electron will be thermally excited across the gap. Additional tunneling measurements (9, 10) of the gap at low temperature have given 23 meV for Δ . There appear to be no infrared measurements of the gap in this material.

The foregoing spectra demonstrate a gap in a "band." The nature of this band is not yet clear. Previous measurements by angle-resolved photoemission band-mapping (11, 12) showed several deeper-lying bands in

general agreement with band calculations, but the bands near the Fermi level were not in agreement with calculated normal-state, one-electron bands (13, 14). (Those band-mapping studies had inadequate resolution for the study of Fermi edge effects.) The orientation of our sample was such that our spectra sample a region in k -space not along a symmetry line, hence not displayed in band calculations. These points are shown in Fig. 3 [from Massida *et al.* (13)], where it can be seen that they are, indeed, near bands that pass through the Fermi level. The states at the Fermi level are, from the calculation (13) a mixture of O-2*p* and Cu-3*d* at the points labeled a and b in the Fig. 3, O-2*p* and Bi-6*s* and 6*p* around the point e, while in the shaded region, Bi-6*s* and *p* states are hybridized with the Cu and O states. A recent angle-integrated photoemission study (15) showed that at the Fermi level, the states are about 35% Cu-3*d* and 65% O-2*p* in character, a conclusion different from that of earlier studies (12, 16). In an angle integrated study, the anticipated Bi component will be difficult to identify, if present. At 18° we are near two calculated bands at the Fermi level, one with a Bi component, but this measurement is not sufficient to confirm the Fermi surface. It is clear that more data are needed to determine if the electronic structure of this material is well described by the band calculations, and with the small Brillouin zone, higher angle resolution (2), with no loss of energy resolution, is desirable. The observed peak and its temperature dependence appear not to be consistent with what is expected to date for photoemission from a resonating valence bond (RVB) model (17). Above T_c this model appears to predict, for an angle-integrated EDC, an edge similar to a Fermi edge, but of different slope, and displaced from the position of the Fermi edge by an amount depending on the maximum spinon energy. Our comparisons of the Fermi edges of Pt and Bi₂Sr₂Ca-Cu₂O₈, the latter in an angle-resolved EDC, indicate no relative shift of the edges above T_c . No RVB predictions for photoemission below T_c have appeared in the literature.

REFERENCES AND NOTES

1. J.-M. Imer *et al.*, *Phys. Rev. Lett.* **62**, 336 (1989).
2. R. Manzke, T. Buslaps, R. Claessen, J. Fink, *Europhys. Lett.*, **9**, 477 (1989)
3. R. S. List *et al.*, *J. Vac. Sci. Tech.*, in press.
4. R. S. List *et al.*, *J. Appl. Phys.*, in press.
5. Cleaving apparently results in a Bi-O surface plane. See P. A. P. Lindberg *et al.*, *Phys. Rev. B* **39**, 2890 (1989).
6. C. G. Olson, *Nucl. Inst. Methods A* **266**, 205 (1988).
7. T. C. Chiang, J. A. Knapp, M. Aono, D. E. Eastman, *Phys. Rev. B* **21**, 3515 (1980).
8. M. Lee *et al.*, *ibid.* **39**, 801 (1989).
9. Y. Chen, H. Tao, S. Zhao, Y. Yan, Q. Yang, *Mod. Phys. Lett. B* **2**, 903 (1988).

10. S. Zhao, H. Tao, Y. Chen, Y. Yan, Q. Yang, *Solid State Commun.* **67**, 1179 (1988).
11. T. Takahashi *et al.*, *Nature* **334**, 691 (1988); *Phys. Rev. B* **39**, 6636 (1989).
12. F. Minami, T. Kimura, S. Takekawa, *ibid.*, p. 4788.
13. S. Massida, J. Yu, A. J. Freeman, *Physica C* **152**, 251 (1988).
14. H. Krakauer and W. E. Pickett, *Phys. Rev. Lett.* **60**, 1665 (1988).
15. R. S. List *et al.*, *Physica C*, in press.

16. Z.-X. Shen *et al.*, *Phys. Rev. B* **38**, 7152 (1988).
17. Y. Chang *et al.*, *ibid.*, **B 39**, 7313 (1989).
18. The Ames Laboratory is operated for USDOE by Iowa State University under contract W-7405-eng-82. Argonne National Laboratory is operated for USDOE under contract W-31-109-ENG-38. The Synchrotron Radiation Center is supported by NSF under contract DMR8601349.

4 May 1989; accepted 21 June 1989

Origins and Movement of Fluids During Deformation and Metamorphism in the Canadian Cordillera

BRUCE E. NESBITT AND KARLIS MUEHLENBACHS

Stable isotope data from quartz veins in the Canadian Cordillera indicate that crustal fluids were heterogeneous in terms of sources and flow paths during Mesozoic-Cenozoic metamorphism and deformation. In regions of strike-slip and extensional faulting, the fluid regime to depths of at least 15 kilometers was dominated by convected, chemically evolved meteoric water. In contrast, in thrust faulted regions, the fluid regime was dominated by fluids derived from metamorphic devolatilization reactions. Deep convection of meteoric water implies that fluid pressures are hydrostatic in such systems not lithostatic, as had been commonly assumed. The occurrence of significantly lower fluid pressures would necessitate reevaluation of the manner in which metamorphic phase equilibria and stress relations in the crust are modeled. In addition, this study indicates that mesothermal gold deposits in the Canadian Cordillera are a product of the meteoric water convection process.

THE EXTENT OF PENETRATION OF surficial waters into the crust is a key question in studies of fluids in the earth's crust (1). Calculations of the probable depth of convection of surficial fluids (2-4) have shown that in rock units with bulk permeabilities of 10^{-17} m² or greater, fluids originating at the surface can move by free convection under a normal geothermal gradient. Data of Brace (5, 6) suggest that permeabilities in excess of 10^{-17} m² are common in the brittle crust, especially in units that have undergone even minor amounts of fracturing. Permeabilities on the order of 10^{-16} m² have been observed to depths of 10 km in the Kola deep hole in the Soviet Union (7). These results indicate that convection of surface waters should be common in the brittle crust, providing that there is a high degree of vertical interconnectivity of fractures. Fluid pressures in petroleum exploration and development wells in actively subsiding sedimentary basins in the U.S. Gulf Coast and elsewhere, however, commonly exceed the hydrostatic head for that depth (1). The presence of these overpressured zones prevents the influx of surface waters. These results have been thought by many to indicate that surface fluids only penetrate a few kilometers into the crust and that the dominant source of deeper fluids in the crust is from expelled pore fluids at shallow depths and from diagenetic or metamorphic devolatilization reactions at greater

depths (1, 8). Unresolved as yet, however, is the question of how generally applicable to other geological settings is the depth-fluid pressure relation observed in these subsiding basins.

The recognition that crustal fluids differ in oxygen and hydrogen isotopic ratios has permitted the common use of stable isotopes to identify the types of fluids involved in various geological processes. Isotopic ratios of meteoric water (rain and snow) vary with latitude and elevation, lower $\delta^{18}\text{O}$ and δD contents being indicative of higher latitudes or elevations or both (9) (Fig. 1). Isotopic values for waters produced by metamorphic or magmatic devolatilization processes are typically less variable and relatively enriched in ^{18}O and D (Fig. 1) (10). Stable isotope studies of both in-place and obducted samples of the oceanic crust (11, 12) have clearly documented that extensive convection of sea water occurred in the oceanic crust to depths of at least 5 km. Recently, evidence of deep convection of sea water also has been obtained from metamorphosed, continental crustal rocks in the Pyrenees (13). The convection of meteoric water in and around igneous plutons in the continental crust has been documented by the work of Taylor and co-workers (14). They have shown that the heat of cooling

Department of Geology, University of Alberta, Edmonton, Alberta T6G 2E3.